Ion Sources and Injectors for HIF Induction Linacs

J. W. Kwan[a*], L. Ahle[b], D.N. Beck[a], F. M. Bieniosek[a], A. Faltens[a], D. P. Grote[b], E. Halaxa[b], E. Henestroza[a], W. B. Herrmannsfeldt[c], V. Karpenko[b], T.C. Sangster[b]

[a]Lawrence Berkeley National Laboratory, Berkeley, CA
[b]Lawrence Livermore National Laboratory, Livermore, CA
[c]Stanford Linear Accelerator Center, Stanford, CA

* Corresponding author. Fax: +1 510 486 5392; email: jwkwan@lbl.gov

Abstract

Ion source and injector development is one of the major parts of the HIF program in the USA. Our challenge is to design a cost effective driver-scale injector and to build a multiple beam module within the next couple of years. In this paper, several current-voltage scaling laws are summarized for guiding the injector design. Following the traditional way of building injectors for HIF induction linac, we have produced a preliminary design for a multiple beam driver-scale injector. We also developed an alternate option for a high current density injector that is much smaller in size. One of the changes following this new option is the possibility of using other kinds of ion sources than the surface ionization sources. So far, we are still looking for an ideal ion source candidate that can readily meet all the essential requirements.

1. Introduction

In the USA, the primary approach for heavy ion driven inertial fusion (HIF) is to use ion beam drivers based on high current induction linacs. The driver can have an array of N ≈ 100 parallel ion beams with a final beam energy in the multi-GeV range. The total required beam charge is ≈ 1 mC. For beam pulse length of ≈ 20 μs at the ion source, the beam current is ≈ 50 A. Typical ions of interest for drivers (based on target penetration range) have mass > 100. However, in the near future, lighter ions such as K^+ and Ar^+ can be useful because they provide an opportunity to do experiments at high ion velocities on medium length accelerator facilities during the early development phases. Unless specified otherwise, all beam currents mentioned in this paper are referred to beams of K^+ ions (i.e., M=39 and Z=1). In an electrostatic system, the beam current can be scaled according to the square root of (Z/M) in order to keep the same perveance for other ion species.

High current heavy ion beams have significant space-charge effects, so the current in each beam is limited by the focussing capability of the beam transport system. Several current-voltage scaling laws are summarized in section 2 for guiding the injector design. The traditional approach is to use a low current density ion source to cope with the space charge problem in low energy beam transport. We propose an alternate approach using a large number of high current density miniature beamlets to circumvent the space charge problem and to manipulate beam focussing for a rapid beam envelope matching. The result is an immense reduction in the size and cost of the injector.

At present, the most optimistic scenario for the HIF development plan in US is to start constructing the so-called Integrated Research Experiment (IRE) within a few years [1]. The IRE is supposed to have driver-scaled beam current and the beam will be accelerated up to a few hundred MeV. That means it will need a driver-scale injector. If we assume that the injector cost is 10% of a $1000M driver, the same injector will require 2/3 the budget of a $150M IRE facility. In order to establish an affordable development path, our aim is to find a way to build driver-scale injector for ≤ $20M. In view of the proposed IRE schedule, we would like to build a prototype (that contains 4-16 beams) in 2-3 years from now.

2. Important beam extraction and transport scaling laws

The injector system contains the ion source, the extractor, the ion gun (also known as the pre-accelerator), and the matching section. The following is a summary of the beam transport scaling relationship in the injector.

2.1. Beam extraction from an aperture

The extractor is basically the first part of the ion gun where the charged particle motion is governed by space-charge-limited flow. Ignoring the curvature of the emitter surface, the beam current density in a space-charge-limited flow is given by the Child-Langmuir relationship

$$J_{CL} = \chi \frac{V^{\frac{3}{2}}}{d^2} \qquad (1)$$

where $\chi = (4\varepsilon_o/9)(2q/M)^{1/2}$ with q and M being the charge and mass of the ions respectively, d the extractor length, and V is the extraction voltage. An important rule to consider is how the breakdown voltage V scales with the gap length d. For gaps shorter than ≈1.0 cm, V scales linearly with d whereas for larger gaps V is approximately proportional to the square root of d. This nonlinear relationship is not favorable to large current systems that require very high voltages (and therefore need very long gaps). Furthermore, for a gas source, the residual gas pressure is also a crucial factor in the extraction system. Substituting this square root scaling into the above equation, we find $J_{CL} \sim 1/d^{1.25}$ which means the current density always decreases when the gap length is increased. It is not possible to raise the extraction voltage to regain current density without eventually encountering the breakdown limit.

For a circular aperture with radius a, the extracted beam current is

$$I_{CL} = \pi\chi\left(\frac{a}{d}\right)^2 V^{\frac{3}{2}} \qquad (2)$$

In order to avoid beam optics aberration, the aspect ratio (a/d) is typically < 0.5. This condition implies that for a fixed aspect ratio the maximum extractable beam current depends only on the maximum extraction voltage (in the form of $V^{3/2}$) that can be applied to the extraction gap without causing voltage breakdowns. Thus it is necessary to use large aperture with large gaps but low current density in order to obtain large current from a single beam.

2.2. Beam transport in the ion gun

The ion gun accelerates a beam to a suitable energy before injecting it into the electrostatic quadrupole (ESQ) matching section. In addition, the ion gun must provide sufficient radial force to keep the ion beam from expanding. A typical ion gun design is to use the Pierce type column. Using an Einzel lenses system (accel-decel scheme) can further improve the ion gun focussing capability. The scaling relationship can be understood by using a simple model of balancing the beam's space charge force with the Einzel lens' focussing force, we find

$$J \approx 2\chi\left(\frac{\Delta V}{L}\right)^2 \frac{1}{\sqrt{\Phi}} \qquad (3)$$

where Φ is the ion kinetic energy in volts, ΔV and L are the voltage difference and gap distance between the electrodes respectively. Once again for large size ion gun the current density decreases because ΔV scales according to the square root of L. The focussing capability also diminishes as the beam gains velocity thus limiting the beam energy range of an ion gun.

2.3. Beam current density in an ESQ beam transport system

In an ESQ beam transport channel, the transportable beam current density can be written as [2]:

$$J \approx \chi \left(\frac{V_q}{b}\right) \frac{\sqrt{\Phi}}{b} \qquad (4)$$

where V_q is the quadrupole voltage and b is the bore radius. In contrast to the ion gun, the ESQ focussing capability diminishes at low beam velocity. Thus there is a cross-over point defining the upper energy limit for ion guns and lower energy limit for ESQ's. This cross-over beam energy decreases with increasing beam current in the channel. For example, the cross-over beam energy for 0.5 A of K^+ is about 1.6 MeV.

3. Average current density in an array of ESQ channels

In designing a multiple beam injector for an HIF linac, it is important to consider the average current density J_{ave} which is defined as the total beam current divided by the overall array cross-sectional area. A higher J_{ave} ESQ array requires smaller vacuum vessel, smaller induction core, less pulsed power, but more difficult alignments and tolerances. An ESQ cross-section is shown in Figure 1. The aperture radius (b) is governed by the equation:

$$b = 1.25a + c \quad . \qquad (5)$$

where a is the maximum beam radius and c is the beam clearance (based on an estimate of the beam steering random error and accelerator alignment and machine tolerance limits). The coefficient 1.25 is due to a limitation in the image force from the electrodes. The electrode radius (R_e) is selected to be $1.146b$ in order to eliminate the dodecapole component of the focusing electric field. The maximum transportable beam current can be calculated according to the voltage breakdown scaling and a lattice length for maximum but stable phase advance [3]. Figure 2 shows the J_{ave} as a function of bore radius in an ESQ lattice for various fixed beam clearances. For each fixed clearance there is an optimum aperture radius that produces a maximum average current density. This optimal aperture radius can also be derived analytically as [4]

$$b_{opt} = \frac{(3+\alpha)c}{(1+\alpha)} \qquad (5)$$

where α is the exponent governing the ESQ voltage scaling ($V_q \quad b^{\alpha}$) and typically α = 0.5 for gaps larger than 1 cm. The curves in Figure 2 were calculated for K^+ ion beams at 2 MeV energy. For design purpose, the peaks of the family of curves in Figure 2 are plotted in Figure 3 to show the optimum J_{ave} as a function of the ESQ bore radius. Also shown in Figure 3 is the beam current in each ESQ channel. It is interesting to see how the beam current and current density increase in opposite directions.

Presently the standard HIF induction linac driver concept uses ESQ focusing up to the first few 100 MeV beam energy [1]. A typical example is to consider an array of 84 beams arranged in a 10 x 10 matrix (with 4 channels removed from each corner). For a clearance limit of 1 cm, the ESQ bore radius is 2.33 cm and the array diameter is about 88 cm.

4. Two possible injector design scenarios

4.1. Low current density option

According to the curves in Figure 3, an ESQ channel of 2.33 cm bore radius (corresponds to 1 cm clearance) can transport 0.43 A of beam current. Since the occupied area (see Figure 1) p^2 = 50 cm^2, we found J_{ave} = 8.6 mA/cm^2. If we slightly overfill the channel to get 0.5 A, J_{ave} becomes 10 mA/cm^2. Consider an array of ion sources with an occupancy factor of 20% (i.e. the aperture center to center spacing is twice the aperture diameter), the required emission current density at the source aperture is 50 mA/cm^2. This is not a very difficult number to achieve for ion sources. However, our study shows that the real limits are in the ion gun and the matching section. Figure 4 shows a typical ion gun design produced by the EGUN code. In order to transport a single beam containing 0.5 A of K^+ ion current through the 1.6 MV ion gun with a proper convergence, the beam current density at the ion source emitting surface must be less than 3.25 mA/cm^2. Since the beam current in each ESQ channel is supplied by a corresponding channel in the injector, the significant difference in the J_{ave} between the ion source (or the ion gun) array and the ESQ array means the two sections will have very different transverse dimensions.

The matching section has two functions: it transforms a round beam (from the ion gun) into an elliptical shaped one (in an ESQ channel) and it compresses the beam envelopes to match the ESQ lattice in the induction linac. Beam envelopes in the matching section are shown in Figure 5. Unfortunately, the beam envelope has a maximum excursion at the 2nd quadruple, corresponding to a minimum J_{ave}, so the required bore diameter at the 2nd quadruple will set the scale length for the entire matching section.

A preliminary 84-beam injector design based on this low current density option has been reported last year [5]. Figure 6 is a schematic diagram of the outermost beamline in the 84-beam array. Note that the beamline is not straight because at the end of the injector all beamlines are parallel to the axis. So it is necessary to steer the beam for a "soft landing". Beam steering is done by dipole field produced by specially shaped (non-circular) ESQ electrodes. The overall dimension of the array is about 3.0 m diameter at the ion source end, 1.0 m diameter at the exit end, 6.0 m long and has the shape of a funnel. Additional space must be allowed between the vacuum vessel and the ion sources for holding the 1.6 MV high voltage.

An alternate matching section designed was proposed to steer the beams slowly using a small offset between each ESQ lattice [6]. In this case, the ESQ electrodes are simple parallel round rods. This system has less beam optical aberrations, however the matching section has become 14 m long.

4.2. High current density option

According to the scaling laws described in section 2, high current density can only be achieved by small low current beamlets. In this section, we describe a conceptual design of a compact multiple beam injector using thousands of high current density miniature beamlets. This approach is similar to that used in developing high energy neutral beam injectors for tokamaks [7, 8]. At low energy where the space charge effect is strong, the beamlets are contained within the pre-accelerator grids. After accelerating the beamlets to ≈ 1 MeV energy, clusters of beamlets will be merged together to form multiple beams of ≈ 0.5 A each. Figure 7 shows the optics design of a 1.2 MV ion gun for a miniature beamlet with 100 mA/cm^2 at the source aperture [9]. The aperture diameter was limited to ≤ 2.5 mm by the focusing capability of the Einzel lens system at the high energy end. Thus each miniature beamlet carries 5 mA (of K^+) and a cluster of 100 beamlets is needed to produce a 0.5 A beam. Figure 8 is a schematic diagram of the pre-accelerator.

With independent control of aiming individual beamlets, we can produce an elliptical beam spot (as oppose to a circular one) at the entrance of the ESQ channel, thus performing beam merging and envelope matching simultaneously. The beam envelopes of the merged beam are shown in Figure 9. This special "asymmetric focusing" scheme greatly simplifies the matching condition downstream; and therefore it nearly eliminates the conventional matching section.

The most critical issue in this high current density approach is the emittance growth due to beam merging. Our design incorporates 3 features to minimize the emittance growth: (1) use a large number of beamlets (≥ 100); (2) let the beamlet merging takes place at energy ≥ 1.2 MeV; (3) geometrically aim the beamlets inward to produce a strong focussing effect and to minimize the length of the merging region. Figure 10 shows the emittance growth and how it reaches equilibrium in about 10 m after entering the ESQ channel in the linac [9]. In the simulation, the 100 beamlets (as shown

in Figure 9) have a total current of 0.5 A and occupy 7% of the grid area. The final beam emittance is 0.85 π-mm-mrad if each beamlet has an initial emittance of 0.005 π-mm-mrad. Interestingly when the initial beamlet emittance is raised to 0.01 π-mm-mrad and 0.02 π-mm-mrad, the final emittance only increases to 1.0 π-mm-mrad and 1.2 π-mm-mrad respectively. This effect simply means the emittance growth is dominated by the space charge effect in the merging process and is not very sensitive to the initial ion temperature. This result has not been optimized yet because we have not determined whether the 7% beam occupancy or the number of 100 beamlets are the optimum. According to theory [10], the emittance growth is less if these parameters are larger.

With each beamlet carrying 5 mA and an emittance of 0.01 π-mm-mrad, the brightness ($B \sim I/\varepsilon^2$) of these beamlets is ≈100 times higher than that required in the low current density large diameter beam. The brightness is diminished in the process of beam merging. Thus it is necessary to start with a current density ≈ 100 mA/cm^2 at the aperture.

If the J_{ave} at the ion source, the extractor, the ion gun, and the ESQ channels are all matched, the multiple beam injector will have the same radial size throughout. All the beamlines in the array will be identical and parallel to the axis so no bending is required. For an 84-beam high current density injector, the dimensions of the array (including a matching section but not including the ion source) is approximately 1 m diameter by 1 m long.

5. Ion sources for HIF

The general requirements for HIF ion sources are listed in Table 1. In addition to these parameters, there are other system requirements such as timing jitter, reliability, availability, and geometric compatibility due to the multiple-beam nature of a large array.

In the low current density case, a large diameter ion source is required to produce a single large current (≈0.5 A) beam. In order to meet the emittance requirement, the ion temperature must be extremely low, e.g., a small fraction of an eV. Furthermore in order to achieve good beam optics, the emitter must be a well-defined spherical surface. For a large diameter, this condition can only be met by using a solid emitter surface. The only known solution for the low current density method is to use surface ionization sources such as contact ionizer or alumino-silicate sources. A 17-cm diameter alumino-silicate surface ionization source was developed (as part of the ILSE project) to produce 0.8 A of K^+ ions with an emittance < 1.0 π-mm-mrad [11]; some recent experimental results are being reported [12]. In the long run, the alumino-silicate source may not have a long enough lifetime for HIF driver applications. Further discussion of surface ionization sources for HIF applications can be found in a previous report [13].

A major disadvantage of surface ionization source is that it only produces alkali metal ions. In general alkali metal vapor is difficult to work with and it has many contamination problems. Power efficiency is poor for this type of ion sources because

the emitter must be heated to ≈ 1000 deg C in steady state temperature even though the beam pulse duty factor is ≤ 2 x 10^{-4}.

Table 1. HIF ion source requirements

Beam current per beam	0.5 A
Beam pulse width	20 μs
Beam rise-time	≤ 1 μs
Repetition rate	10 Hz
Ion mass (AMU)	100-200
Charge state purity	> 90%
Emittance (π-mm-mrad, normalized)	< 1.0
Current fluctuation level	≤ 1%
Current profile uniformity	> 95%
Pulse-to-pulse variation	≤ 1%
Beam energy spread	≤ 2 kV
Lifetime	10^8 pulses

In the high current density case, the ion source requirements can be met by ion sources other than the surface ionization type [14]. In principle, the surface ionization sources can deliver current density up to 100 mA/cm^2 if the emitter temperature can reach > 1250 deg C. More than likely the problem lies in the neutral atom evaporation being too high at this temperature for continuous operation. The gas discharge sources are more suitable for this application. Recent experiments on these sources have shown current densities much higher than 100 mA/cm^2 and rise time in the order of a few μs [15,16].

Charge exchange is a problem for gas discharge sources. Beam ions colliding with the background gas in the pre-accelerator will produce fast neutrals and slow ions. The fast neutrals can cause more gas desorption which in turn produces more beam loss at the tail end of a 20 μs pulse. The slow ions result in energy dispersion in the beam thus affecting the final focusing at the target. In order to minimize charge exchange, the discharge must be operated at low gas pressure and the pre-accelerator must have efficient vacuum pumping.

The MEVVA source offers other advantages such as simple parts, no gas flow and potentially high charge state ions. Recent results have shown significant improvements in beam reproducibility and beam noise reduction [17]. It is typical for a MEVVA source to produce ions of several different charge states. Only ions of one charge state is useful, the rest are harmful in an induction linac. So a significant effort has been devoted to look for heavy elements that can produce a high percentage (e.g. 90%) of a single charge state [18].

The laser ion sources are in many ways similar to the MEVVA source--no gas, high current, multiple charge states. It is possible that the laser ion source can have a

lower rate of electrode erosion therefore a longer life than MEVVA. Nevertheless, if 84 high power laser beams are needed to operate the 84 ion sources in the injector, then there is a serious issue of cost and reliability for the system. Further research is required to evaluate the laser ion source for HIF induction linac application.

6. Discussion and Summary

Following the traditional way of building injectors for HIF induction linac, we have produced a preliminary design for a multiple beam driver-scale injector. However, we were concerned with its size, storage energy, and cost. Based on the fundamental scaling laws, we determined that a much smaller injector can be built if the beams are divided into miniature beamlets. The key issue is to increase the average current densities at the ion source, pre-accelerator, and matching section in order to match the current density in the ESQ array of the linac. In addition, by aiming the beamlets to produce an elliptical spot at the entrance of the ESQ channel, we have almost eliminated the previously bulky matching section.

One of the changes from this new approach is the possibility of using other kinds of ion sources than the surface ionization sources. So far, we have not chosen an ion source candidate because the ones that have been considered are not readily meeting all the essential requirements. Ion source research and development is a top priority in the near future of the HIF program. A new 500 kV test stand is currently being construct at LLNL specifically for this use [19]. Within the next few years, we are also expected to build a scalable module of a multiple beam injector to demonstrate our readiness for the IRE project.

7. Acknowledgement

This work is supported by the Office of Fusion Energy Science, US DOE under contract No. DE-AC03-76SF00098 (LBNL) and W-7405-ENG-48 (LLNL).

8. References

[1] J.J. Barnard, this proceeding paper ThP.IV-16

[2] E.P. Lee, et al, Proc. of Inter. Symp. on Heavy Ion Inertial Fusion;Fusion Engineering and Design, 32-33, p323, (1996).

[3] J. W. Kwan, et al, Proc. of Inter. Symp. on Heavy Ion Inertial Fusion;Fusion Engineering and Design, 32-33, p299, (1996).

[4] R.O. Bangerter, Proc. of Inter. Symp. on Heavy Ion Inertial Fusion; Nuovo Cimento 1445 (1993).

[5] J.W. Kwan, et al, Proc. Particle Accelerator Conf., New York, March, (1999).

[6] L. Ahle, this proceeding paper ThP.IV-12

[7] T. Inoue, et al., Rev. Sci. Instrum, 66(7), p3859, (1995).

[8] J.W. Kwan, et al, Rev. Sci. Instrum, 66(7), p3864, (1995).

[9] E. Henestroza, this proceeding paper ThP.IV-11

[10] O.A. Anderson, Proc. of Inter. Symp. on Heavy Ion Inertial Fusion; Fusion Engineering and Design, 32-33, p209, (1996)
[11] S. Yu, et al, Proc. of Inter. Symp. on Heavy Ion Inertial Fusion; Fusion Engineering and Design, 32-33, p309, (1996)
[12] F. M. Bieniosek, this proceeding paper ThP.IV-10
[13] J.W. Kwan, W.W. Chupp, and S. Eylon, Proc. Particle Accelerator Conf., p2755, Vancouver, March, (1997).
[14] J.W. Kwan, Proc. of Inter. Symp. on Heavy Ion Inertial Fusion; Nucl. Instrum. and Methods in Phys. Research A, 415, p268, (1998)
[15] L.T. Perkins, et al, Rev. Sci. Instrum. 69(2), p1060, (1998).
[16] J. Reijonen, et al, Proc. Particle Accelerator Conf., New York, March, (1999).
[17] F. Liu, et al, Rev. Sci. Instrum. 69(2), p819, (1998).
[18] A. Anders, this proceeding paper ThP.IV-05
[19] T. C. Sangster, this proceeding paper ThP.IV-14

Figure Captions

Fig. 1. Cross section of an ESQ
Fig. 2. Average current density of an ESQ array for K^+ ion beams at 2 MeV.
Fig. 3. Average current density and beam current for an ESQ channel with $b = 2.33c$.
Fig. 4. Ion gun design for a low current density 0.5 A K^+ beam.
Fig. 5. Beam envelopes in the ESQ matching section (low J_{ave} case).
Fig. 6. Schematic diagram of the outer most beamline in the matching section.
Fig. 7. An ion gun design for a 5 mA, 1.2 MeV K^+ beamlet.
Fig. 8. Schematic diagram of the multiple beamlet pre-accelerator with a merging section/matching section.
Fig. 9. Beam envelopes of merging beamlets and matching into an ESQ channel.
Fig. 10. Emittance growth due to beamlet merging and matching.

Fig. 1. Cross section of an ESQ

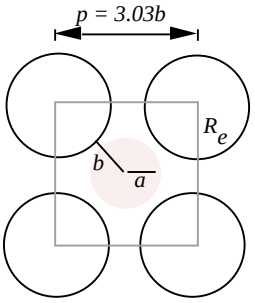

Fig. 2. Average current density of an ESQ array for K^+ ion beams at 2 MeV.

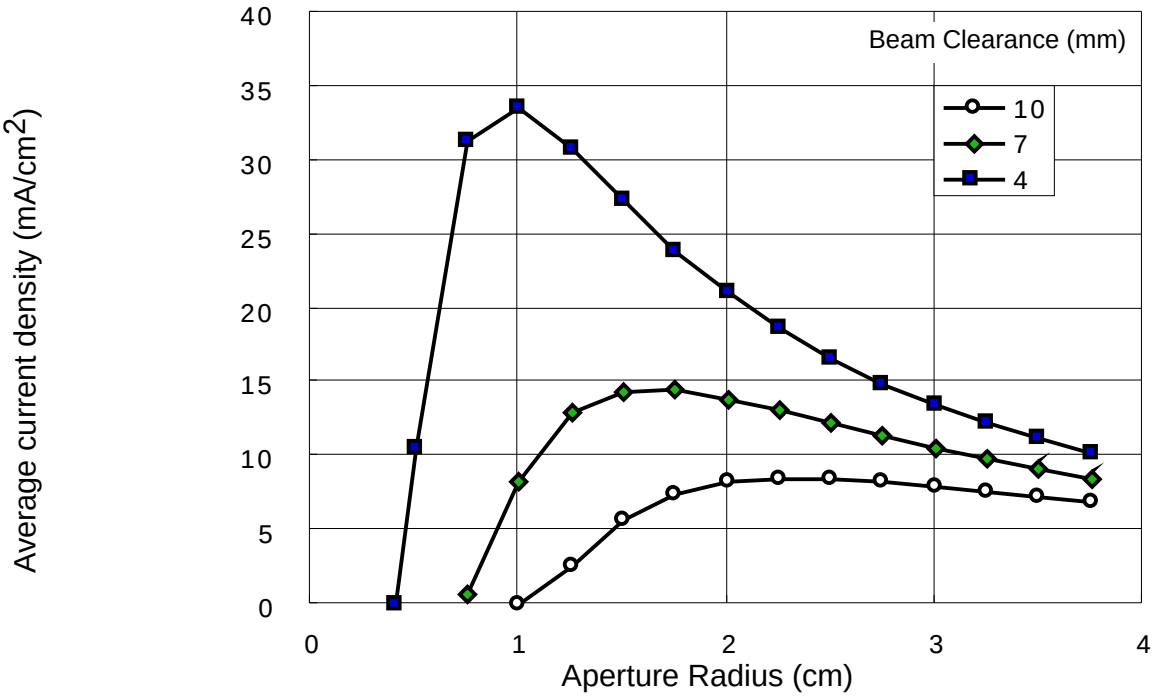

Fig. 3. Average current density and beam current for an ESQ channel with $b = 2.33c$.

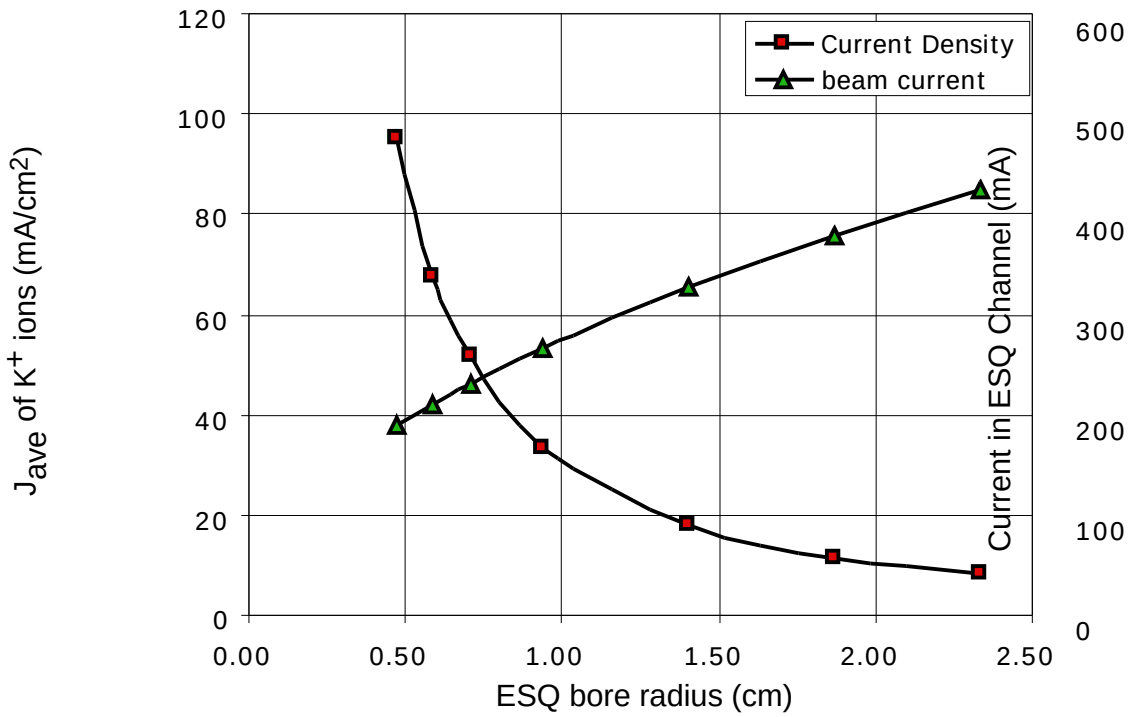

Fig. 4. Ion gun design for a low current density 0.5 A K^+ beam.

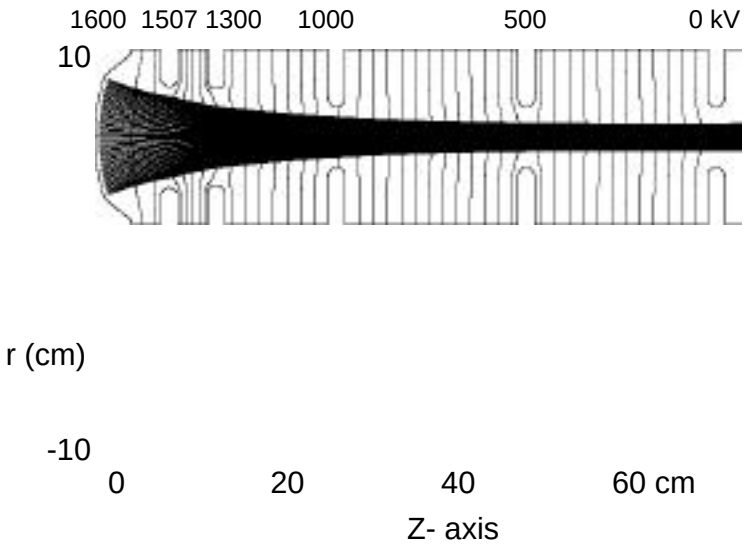

Fig.5. Beam envelopes in the ESQ matching section (low J_{ave} case).

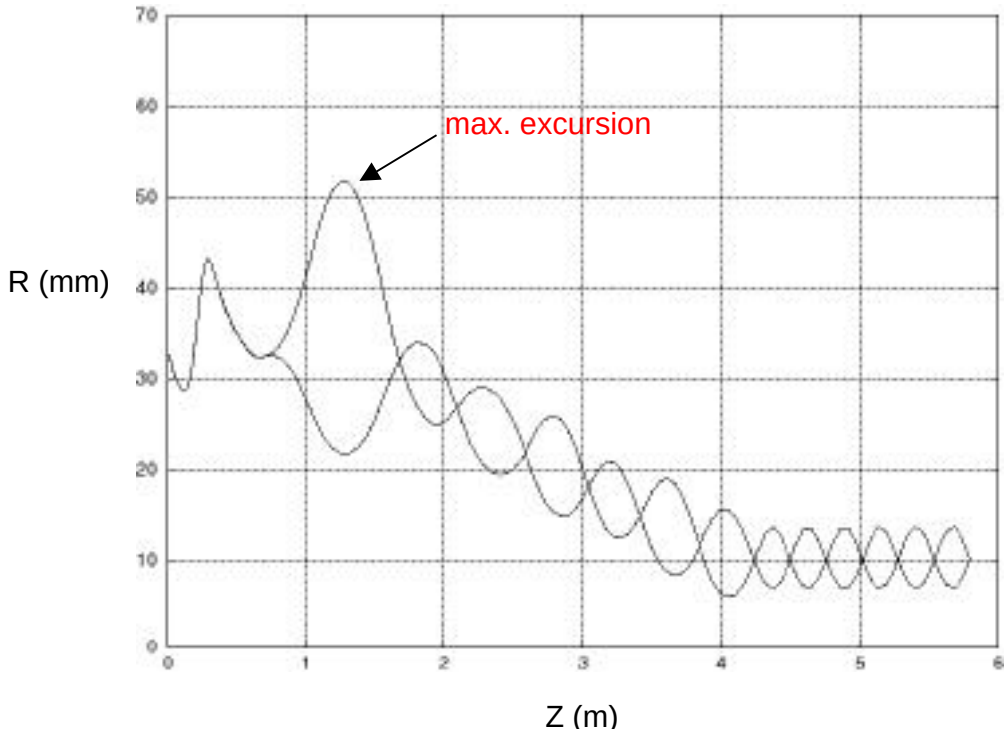

Fig. 6. Schematic diagram of the outer most beamline in the matching section.

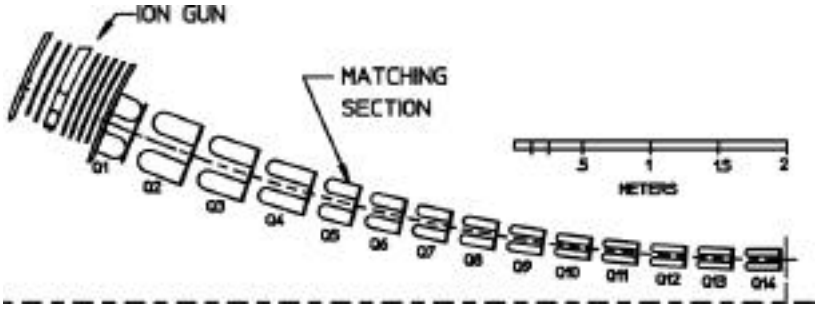

Fig. 7. An ion gun design for a 5 mA, 1.2 MeV K^+ beamlet.

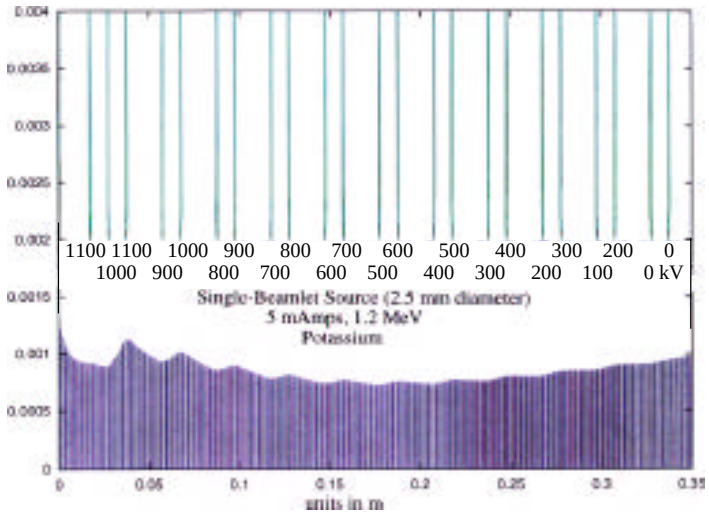

Z (m)

Fig. 8. Schematic diagram of the multiple beamlet pre-accelerator with a merging section/matching section.

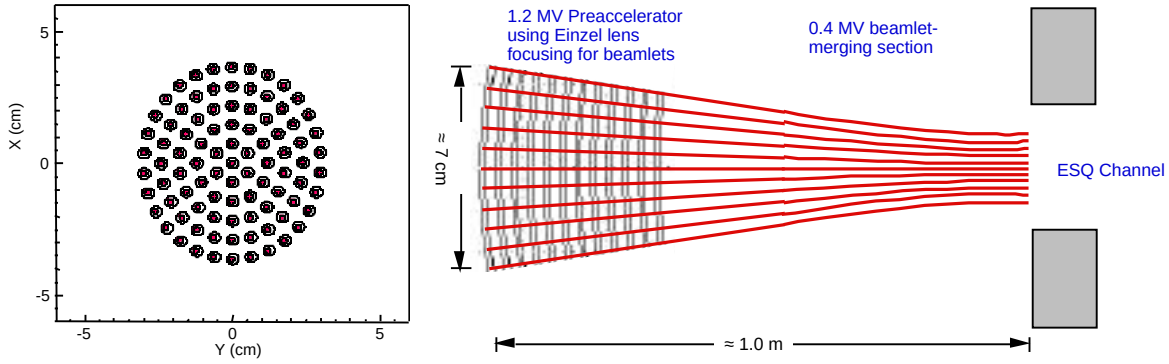

Fig. 9. Beam envelopes of merging beamlets and matching into an ESQ channel.

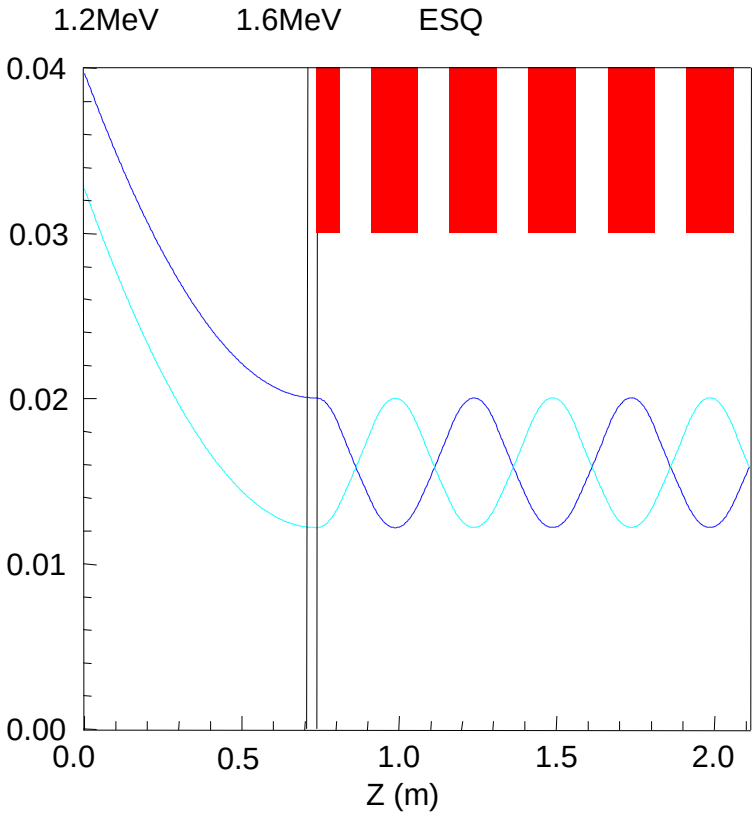

Fig. 10. Emittance growth due to beamlet merging and matching.